  Bull. Chem. Soc. Jpn., 63, 2281—2287 (1990)

The Crystal and Band Electronic Structures of Bis[4,5-ethylenedithio-4′,5′-(vinylenedithio)tetrathiafulvalenium] Hexafluorophosphate, and Hexafluoroarsenate [EVT_2PF_6 and EVT_2AsF_6]

Hideyuki NAKANO, Kenji MIYAWAKI, Takashi NOGAMI,*,† Yasuhiko SHIROTA, Shigeharu HARADA, Nobutami KASAI, Akiko KOBAYASHI,†† Reizo KATO,††† and Hayao KOBAYASHI†††

Department of Applied Chemistry, Faculty of Engineering, Osaka University, Yamadaoka, Suita, Osaka 565

††Department of Chemistry, Faculty of Science, The University of Tokyo, Hongo, Bunkyo-ku, Tokyo 113

†††Department of Chemistry, Faculty of Science, Toho University, Funabashi, Chiba 274

(Received November 16, 1989)

The molecular and crystal structures of EVT_2PF_6 and EVT_2AsF_6 [EVT=4,5-ethylenedithio-4′,5′-(vinylenedithio)tetrathiafulvalene] were determined by an X-ray diffraction method. Tight-binding band-structure calculations were made, and the results were compared with those of closely resembling conducting salts, α-(BEDT-TTF)$_2PF_6$ and VT_2PF_6 [BEDT-TTF=bis(ethylenedithio)tetrathiafulvalene; VT=bis(vinylenedithio)tetrathiafulvalene]. It was concluded that the extent of the two-dimensional nature of the band electronic structure increased systematically in the order VT_2PF_6, EVT_2PF_6, and α-(BEDT-TTF)$_2PF_6$; this result was analysed in terms of their crystal structures.

Studies concerning conducting organic salts have led to various organic superconductors during the last few years.[1] The properties of conducting salts are closely related to their crystal structures. Although the existence of organic superconductors with two-dimensional molecular arrangements has been established,[2] most of the conducting salts have a stack of donor and/or acceptor molecules in the crystal to form a columnar structure. It has now been recognized that an intercolumnar interaction through chalcogen-chalcogen contacts shorter than the van der Waals distance plays an important role in realizing the two-dimensional electrical properties of conducting salts. This is believed to be effective for suppressing the Peierls transition inherent in a one-dimensional system. In order to determine the effect of a slight modification of a donor molecule on both the crystal and band electronic structures of a conducting salt, it is important to compare the crystal and band electronic structures of salts possessing similar molecular structures at the donor site. Knowledge obtained in this way will be useful in designing new conducting organic salts. For this purpose we noticed bis(ethylenedithio)tetrathiafulvalene (BEDT-TTF), 4,5-ethylenedithio-4′,5′-(vinylenedithio)tetrathiafulvalene (EVT),[3] and bis(vinylenedithio)tetrathiafulvalene (VT)[4] to be donor molecules possessing similar molecular structures. We carried out X-ray crystallographic studies of EVT_2PF_6 and EVT_2AsF_6. Band electronic calculations were made based on a tight-binding method, using the molecular orbitals obtained by an extended Hückel method.[5] These results were compared with those of α-(BEDT-TTF)$_2PF_6$ and VT_2PF_6, which have the same crystal system and space group (triclinic, $P\bar{1}$)[6,7] as those of EVT_2PF_6 and EVT_2AsF_6. We found that a slight modification of the donor site results in a systematic change of both the crystal and band electronic structures.[8]

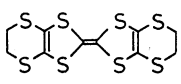

BEDT-TTF

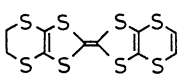

EVT

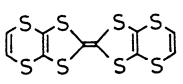

VT

† Present address: Department of Applied Physics and Chemistry, The University of Electro-Communications, Chofugaoka, Chofu, Tokyo 182.

Experimental

Electrochemical Crystallization. EVT was synthesized by a previously reported method.[3] Single crystals of EVT_2PF_6 and EVT_2AsF_6 were grown using an electrochemical crystallization method in tetrahydrofuran and chlorobenzene, respectively, under a galvanostatic condition (~1 μA), using platinum wires as electrodes and tetrabutylammonium hexafluorophosphate or tetrabutylammonium hexafluoroarsenate as electrolytes.

Crystal Data. EVT_2PF_6: $(C_{10}H_6S_8)_2PF_6$, M=910.33, triclinic, $P\bar{1}$, a=6.47(2), b=7.80(3), c=15.81(5) Å, α=94.8(8), β=80.2(3), γ=100.2(6)°, V=772(5) Å^3, Z=1, D_c=1.96 g cm^{-3}, μ(Mo K_α)=11.8 cm^{-1}; EVT_2AsF_6 $(C_{10}H_6S_8)_2AsF_6$, M=954.28, triclinic, $P\bar{1}$, a=6.494(1), b=7.760(2), c=16.039(4) Å, α=94.97(2), β=98.63(1), γ=79.58(2)°, V=784.5(3) Å^3, Z=1, D_c=2.02 g cm^{-3}, μ(Mo K_α)=21.6 cm^{-1}. The crystals were needle shaped with approximate dimensions of 0.78×0.21×0.08 mm^3 for EVT_2PF_6 and 0.53×0.28×0.10 mm^3 for EVT_2AsF_6. X-Ray diffraction data were collected by the θ-2θ scan technique up to 2θ=47° and 50° for EVT_2PF_6 and EVT_2AsF_6 respectively on a Rigaku AFC-4 four-circle diffractometer, using graphite monochromatized Mo K_α radiation (λ=0.71069 Å). The scan rates (θ) were 2° min^{-1} for EVT_2PF_6 and 4° min^{-1} for EVT_2AsF_6, and the scan widths $\Delta\theta$=(1.2+0.5 tan θ)° for EVT_2PF_6 and $\Delta\theta$=(1.0+0.5 tan θ)° for EVT_2AsF_6. Backgrounds were counted for 5 s at both ends of each scan. No significant intensity decay of three standard reflections, which were measured after every 100 reflections, were detected for either crystal. For EVT_2PF_6, of the 2523 reflections measured, 1778 were observed ($|F_o|>2\sigma(F_o)$). For EVT_2AsF_6, of the 2990 reflections measured, 2565 were observed ($|F_o|>2\sigma(F_o)$). The data were corrected for both

Lorentz and polarizaion factors, but not for absorption.

The structures were solved by a direct method (MULTAN 78),[9] and were refined anisotropically by a block-diagonal least-squares procedure (HBLS V) for nonhydrogen atoms.[10] Not all of the hydrogen atoms could be reasonably refined. Thus, they were relocated at the calculated positions with the isotropic temperature factors set equal to those of bonded carbon atoms. They were included in the calculations but were not refined. The minimized function was $\Sigma\omega(\Delta F)^2$. The weighting functions used in the final stage of the refinements were $\omega=[\sigma^2(F_o)-0.0045|F_o|+0.0149|F_o|^2]^{-1}$ for EVT_2PF_6 and $\omega=[\sigma^2(F_o)-0.0055|F_o|+0.0029|F_o|^2]^{-1}$ for EVT_2AsF_6. The atomic scattering factors were taken from those of International Tables of X-Ray Crystallography.[11] The final R indices were 0.118 for EVT_2PF_6 and 0.053 for EVT_2AsF_6. The atomic coordinates and equivalent isotropic temperature factors[12] are given in Tables 1 and 2.[13]

Table 1. Atomic Parameters of Nonhydrogen Atoms of EVT_2PF_6, with Equivalent Isotropic Temperature Factors[12]

Atom	x	y	z	B_{eq}/Å^2
C(1)	0.492(2)	0.284(2)	0.5181(8)	2.9
C(2)	0.324(3)	0.151(2)	0.3864(9)	2.9
C(3)	0.532(3)	0.172(2)	0.3609(8)	3.0
C(4)	0.251(3)	−0.005(3)	0.233(1)	5.4
C(5)	0.453(3)	0.092(3)	0.1958(9)	4.2
C(6)	0.525(2)	0.338(1)	0.6009(8)	2.2
C(7)	0.476(2)	0.429(2)	0.7616(8)	2.8
C(8)	0.683(2)	0.461(2)	0.7356(7)	2.1
C(9)	0.537(3)	0.361(2)	0.9149(8)	3.4
C(10)	0.749(3)	0.399(2)	0.8942(8)	3.2
S(1)	0.2399(6)	0.2125(5)	0.4932(3)	3.4
S(2)	0.6982(5)	0.2619(5)	0.4374(2)	3.1
S(3)	0.1193(6)	0.0715(6)	0.3288(3)	3.9
S(4)	0.6658(6)	0.1268(6)	0.2597(3)	4.0
S(5)	0.3166(5)	0.3484(5)	0.6836(2)	3.0
S(6)	0.7766(6)	0.4044(5)	0.6299(2)	2.9
S(7)	0.3599(6)	0.4554(5)	0.8664(3)	3.2
S(8)	0.8696(6)	0.5257(5)	0.8068(3)	3.4
P	0.	0.	0.	2.8
F(1)	0.014(3)	0.201(1)	0.0221(8)	7.8
F(2)	−0.231(1)	−0.012(2)	−0.0213(7)	6.3
F(3)	0.091(2)	0.042(1)	−0.0957(6)	6.0

Table 2. Atomic Parameters of Nonhydrogen Atoms of EVT_2AsF_6, with Equivalent Isotropic Temperature Factors[12]

Atom	x	y	z	B_{eq}/Å^2
C(1)	0.5103(7)	0.2812(6)	0.5211(3)	3.0
C(2)	0.6771(7)	0.1498(6)	0.3899(3)	3.0
C(3)	0.4687(7)	0.1710(6)	0.3641(3)	3.1
C(4)	0.753(1)	−0.010(2)	0.2363(4)	6.4
C(5)	0.5489(8)	0.0923(7)	0.2004(3)	4.2
C(6)	0.4759(7)	0.3398(6)	0.6010(3)	2.8
C(7)	0.5221(7)	0.4333(6)	0.7591(3)	2.7
C(8)	0.3148(7)	0.4601(6)	0.7351(3)	2.8
C(9)	0.4610(8)	0.3674(7)	0.9131(3)	3.6
C(10)	0.2506(9)	0.4059(7)	0.8913(3)	4.1
S(1)	0.7610(2)	0.2141(2)	0.4940(1)	3.5
S(2)	0.3041(2)	0.2623(2)	0.4391(1)	3.4
S(3)	0.8839(2)	0.0699(2)	0.3313(1)	4.2
S(4)	0.3384(2)	0.1227(2)	0.2639(1)	4.3
S(5)	0.6831(2)	0.3508(2)	0.6821(1)	3.3
S(6)	0.2233(2)	0.4054(2)	0.6298(1)	3.1
S(7)	0.6390(2)	0.4593(2)	0.8640(1)	3.7
S(8)	0.1280(2)	0.5299(2)	0.8049(1)	3.8
As	0.	0.	0.	3.2
F(1)	−0.0076(9)	0.2184(5)	0.0208(3)	8.7
F(2)	0.2481(5)	−0.0220(7)	−0.0259(3)	7.5
F(3)	−0.1007(6)	0.0351(6)	−0.1027(2)	6.4

Electrical Conductivities. The temperature dependences of the electrical conductivities of the single-crystals of EVT_2PF_6 and EVT_2AsF_6 were measured by a four-probe method, using a D-type Cryomini Refrigerator (Osaka Sanso Co. Ltd).

Results and Discussion

Electrical Conductivities. Figure 1 shows the temperature dependence of the electrical conductivities of EVT_2PF_6 and EVT_2AsF_6 along the b-axis. The electrical conductivities of EVT_2PF_6 and EVT_2AsF_6 at room temperature were 0.76 S cm^{-1} and 0.17 S cm^{-1}, respectively. They showed a semiconducting behavior with small activation energies of ca. 0.14 eV for EVT_2PF_6 and 0.11 eV for EVT_2AsF_6. α-(BEDT-TTF)$_2PF_6$ also showed a semiconducting behavior with a similar band gap of about 0.1 eV.[6] On the

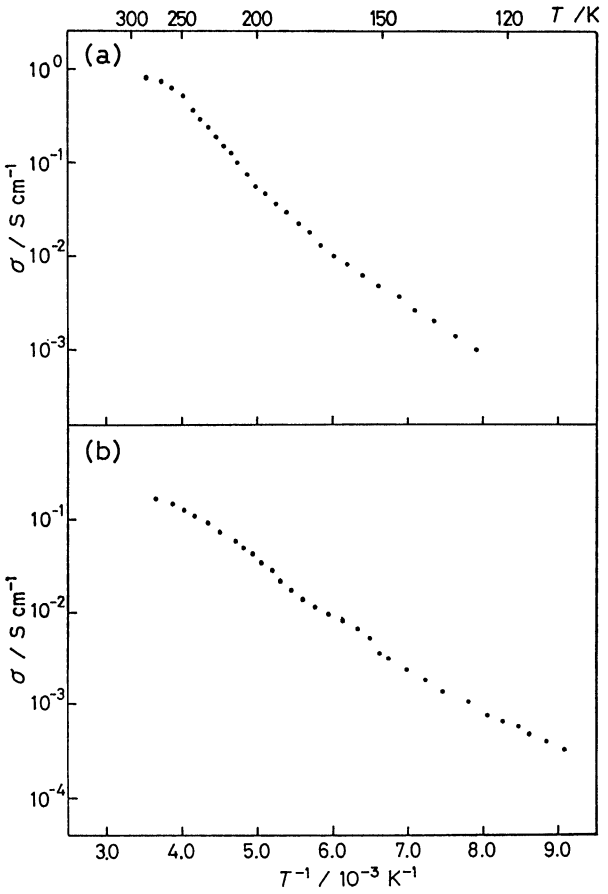

Fig. 1. Temperature dependences of the electrical conductivities of the single crystals of EVT_2PF_6 and EVT_2AsF_6 measured by a four probe method. (a) EVT_2PF_6, (b) EVT_2AsF_6.

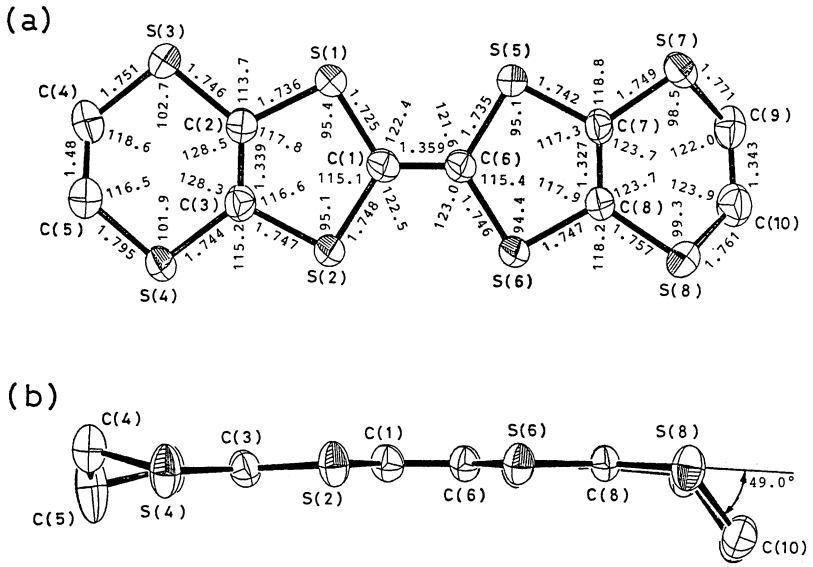

Fig. 2. The molecular structure of EVT molecule in EVT_2AsF_6, and the bond lengths and bond angles. (a) Over view, (b) side view. Nonhydrogen atoms are drawn as thermal ellipsoids with 50% probability level. Estimated standard deviations of the bond lengths and angles are 0.005—0.02 Å and 0.3—0.6° respectively.

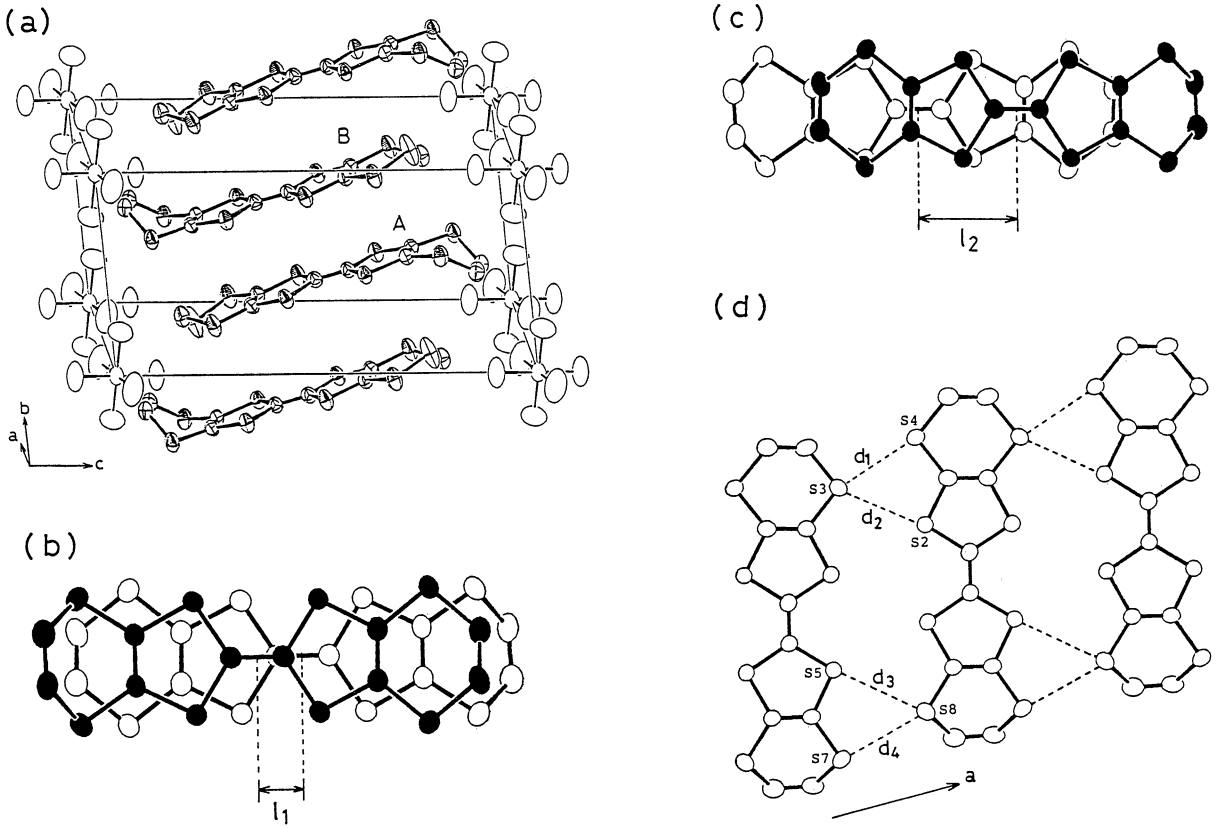

Fig. 3. (a) The crystal structure of EVT_2AsF_6. The molecules A and B are related by the symmetry operation $(1-x, 1-y, 1-z)$. (b) The mode of a stacking of EVT molecules related by the symmetry operation $(1-x, 1-y, 1-z)$. (c) The mode of a stacking of EVT molecules related by the symmetry operation $(1-x, -y, 1-z)$. (d) The arrangement of the EVT molecules along the a-axis. The dotted lines indicate the S···S contacts shorter than the van der Waals distance (3.7 Å). The values of l_1, l_2, d_1, d_2, d_3, and d_4 are summarized in Table 3.

other hand, VT_2PF_6 showed a metallic behavior above 180 K, below which the conductivity was activated (E_a~0.055 eV (T<100 K)).[7]

Molecular and Crystal Structures of EVT_2AsF_6 and EVT_2PF_6. Figure 2 shows the molecular structure of the EVT molecule in the EVT_2AsF_6 crystal, together with the bond lengths and bond angles. The planarity of the EVT molecule was increased in its semication state ($EVT^{+0.5}$).[3] No conformational disorder was found at the ethylene group of the EVT molecule. Figure 3 shows the crystal structure of EVT_2AsF_6. Only one EVT molecule is crystallographically independent, and the AsF_6^- anion is on the center of symmetry. The EVT molecules are stacked along the b-axis, as is usually observed for the conducting salts of TTF derivatives (Fig. 3(a)). Two kinds of the molecular overlap shown in Figs. 3(b) and 3(c) are observed. In one overlap mode (Fig. 3(b)), two EVT molecules are slightly shifted relative to each other within the unit cell. In the other overlap mode (Fig. 3(c)), the five-membered ring of one EVT molecule is overlapped with the six-membered ring of another EVT molecule across the unit cell. These two overlap modes are characterized by l_1 and l_2 in Figs. 3(b) and 3(c). No intermolecular S····S contact shorter than the van der Waals distance (3.7 Å) was found within the donor column. This fact is in contrast with the crystal structures of α-(BEDT-TTF)$_2PF_6$ and VT_2PF_6; intermolecular S····S contacts shorter than 3.7 Å were found within the donor column for these salts.[6,7] Table 3 shows the relative shifts of the donor molecules (l_1 and l_2) and intercolumnar S····S distances (d_1, d_2, d_3, and d_4) in α-(BEDT-TTF)$_2PF_6$, EVT_2PF_6, EVT_2AsF_6, and VT_2PF_6 for the sake of a comparison (see also Figs. 3(b), 3(c), and 3(d)). All of the S····S contacts along the a-axis were shorter than 3.7 Å in EVT_2AsF_6, as shown in Fig. 3(d) and Table 3. Both α-(BEDT-TTF)$_2PF_6$ and VT_2PF_6 also possess intercolumnar S····S contacts shorter than 3.7 Å.[6,7] The molecular and crystal structures of EVT_2PF_6 were found to be very similar to those of EVT_2AsF_6. Hence, the above arguments regarding the molecular and crystal structures of EVT_2AsF_6 are also applicable to the case of EVT_2PF_6. However, the final R value

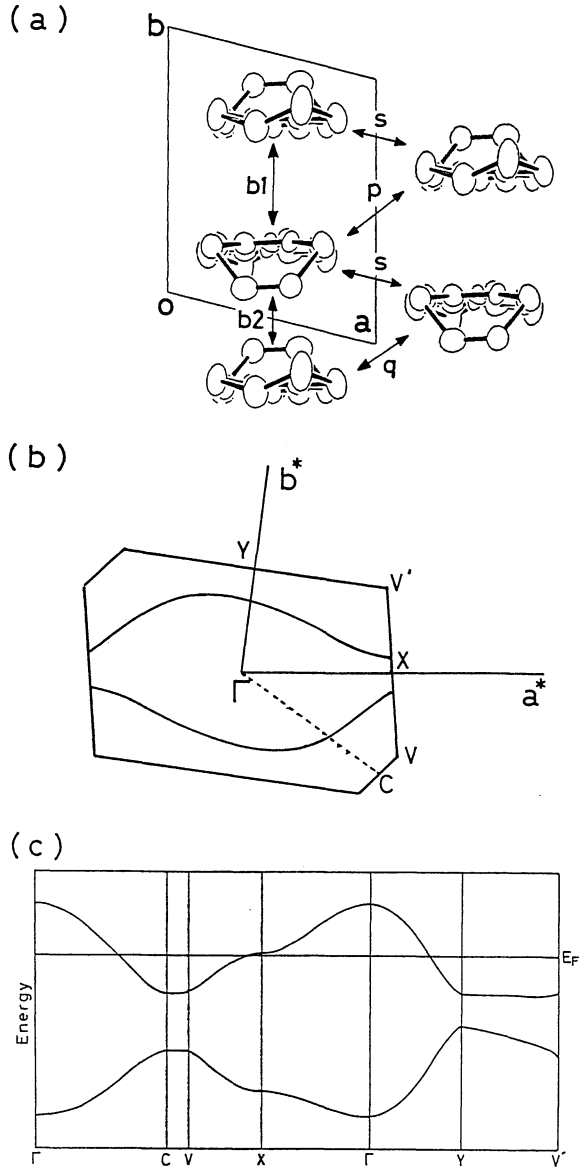

Fig. 4. (a) Intermolecular overlap integrals ($b1$, $b2$, p, q, and s), (b) Fermi surface, and (c) band structure of EVT_2PF_6. Since this salt shows a semiconducting behavior, the absence of the band gap (in other words, the appearance of the Fermi surface) will be caused by the neglect of on-site Coulomb repulsion among conducting electrons in the present calculation.

Table 3. Relative Shift of Donor Molecules (l_1 and l_2) and Intercolumnar S···S Distances between Donor Molecules (d_1, d_2, d_3, and d_4) in the Crystals of α-(BEDT-TTF)$_2PF_6$, EVT_2PF_6, EVT_2AsF_6, and VT_2PF_6

Distances[a] /Å	α-(BEDT-TTF)$_2PF_6$	EVT_2PF_6	EVT_2AsF_6	VT_2PF_6
l_1	0.3	1.2	1.2	1.6
l_2	4.2	3.0	3.0	2.4
d_1	3.48	3.404(7)	3.394(3)	3.51
d_2	3.61	3.450(6)	3.503(2)	3.56
d_3	3.57	3.619(5)	3.664(2)	3.71
d_4	3.58	3.599(6)	3.592(2)	3.43

a) The distances l_1, l_2, d_1, d_2, d_3, and d_4 are shown in Figs. 3(b), 3(c), and 3(d) for EVT_2AsF_6 as typical examples.

Table 4. Intermolecular Overlap Integrals of HOMO Calculated by an Extended Hückel Molecular Orbital Method[a)]

Overlap integral	α-(BEDT-TTF)$_2$PF$_6$	EVT$_2$PF$_6$	EVT$_2$AsF$_6$	VT$_2$PF$_6$
$b1\times10^3$	20.2	14.5	14.5	13.2
$b2\times10^3$	8.7	8.4	8.6	13.9
$p\times10^3$	2.9	1.8	1.6	2.1
$q\times10^3$	0.6	3.0	3.3	1.3
$s\times10^3$	−2.5	−1.0	−0.8	−1.4

a) Overlap integrals *b1*, *b2*, *p*, *q*, and *s* are shown in Fig. 4 for EVT$_2$PF$_6$ as a typical example.

of the latter-mentioned salt was large (R=0.118) due to poor crystal quality.

Band Electronic Structures. Figure 4 shows intermolecular overlap integrals, Fermi surface, and the band structure of EVT$_2$PF$_6$ calculated by a tight-binding approximation based on an extended Hückel molecular orbital.[14] The band structure and Fermi surfaces of EVT$_2$AsF$_6$ were very similar to those of EVT$_2$PF$_6$.[15] We also obtained both closed and open Fermi surfaces for α-(BEDT-TTF)$_2$PF$_6$ and VT$_2$PF$_6$,[7] respectively. The appearance of the Fermi surfaces in α-(BEDT-TTF)$_2$PF$_6$, EVT$_2$PF$_6$, and EVT$_2$AsF$_6$ conflicts with their semiconducting properties. These contradictory results are caused by an on-site Coulomb repulsion among conducting electrons, which was not taken into account in the present calculation. Since the present calculation method gives a simple perspective concerning the dimensionality of many conducting organic salts,[16] the following analysis is believed to be valid for any discussion about the relative band electronic structures of BEDT-TTF-, EVT-, and VT- salts. The values of intermolecular overlap integrals of HOMO levels in VT$_2$PF$_6$, EVT$_2$PF$_6$, EVT$_2$AsF$_6$ and α-(BEDT-TTF)$_2$PF$_6$ are summarized in Table 4. Here, the intermolecular overlap integrals (*b1*, *b2*, *p*, *q*, and *s*) in EVT$_2$PF$_6$ are shown in Fig. 4 as a typical example. The amount of the intermolecular transfer integral (t) is assumed to be of the order of $t\approx ES$ [E=orbital energy of HOMO level (~−8.5 eV); S=intermolecular overlap integral]. Table 4 shows that a dimeric intermolecular interaction exists in the direction of the donor stack in α-(BEDT-TTF)$_2$PF$_6$; *b1* is more than twice as large as *b2*. The ratio of *b1*/*b2* decreases systematically in the order α-(BEDT-TTF)$_2$PF$_6$>EVT$_2$PF$_6$>VT$_2$PF$_6$. Thus, an almost homogeneous intermolecular interaction within the donor column was found for VT$_2$PF$_6$ ($b1\approx b2$). This feature makes the effective band width of VT$_2$PF$_6$ the largest among these salts; this is related to the fact that only VT$_2$PF$_6$ shows a metal-like behavior. α-(BEDT-TTF)$_2$PF$_6$ has a much larger absolute value of the overlap integral $|s|$ than those of the other salts; s is a measure of the side-by-side intermolecular interaction. The dimensionality of the band electronic structure of these salts is discussed below from the viewpoint of their conduction band widths.

Table 5. Relative Conduction Band Widths[17,18)] of α-(BEDT-TTF)$_2$PF$_6$, EVT$_2$PF$_6$, EVT$_2$AsF$_6$, and VT$_2$PF$_6$

Salts	$\Delta W_{\Gamma\text{-Y}}$	$\Delta W_{\Gamma\text{-X}}$
α-(BEDT-TTF)$_2$PF$_6$	18.6	17.0
EVT$_2$PF$_6$	22.8	13.6
EVT$_2$AsF$_6$	23.8	13.0
VT$_2$PF$_6$	30.4	12.4

The matrix elements (H_{ij}) of a secular equation of α-(BEDT-TTF)$_2$PF$_6$, EVT$_2$PF$_6$, EVT$_2$AsF$_6$, and VT$_2$PF$_6$ are written as follows (see also Fig. 4):[17,18)]

$$H_{11}=H_{22}=2t_s\cos(ka)$$

and

$$H_{12}=H_{21}^*=t_{b1}+t_{b2}e^{-ikb}+t_p e^{-ikc}+t_q e^{-i(kb+kc)}.$$

Here, t_x (x=*b1*, *b2*, *p*, *q*, and *s*) denote the intermolecular transfer integrals. By solving the secular equation, we obtained the following equations for the conduction-band widths (ΔW), important measures for the dimensionality of the band electronic structures of the conducting salts:

$$\Delta W_{\Gamma\text{-Y}}=-2(t_{b2}+t_q)$$

and

$$\Delta W_{\Gamma\text{-X}}=4t_s-2(t_p+t_q).$$

$\Delta W_{\Gamma\text{-Y}}$ and $\Delta W_{\Gamma\text{-X}}$ are the conduction-band widths in the Γ-Y and Γ-X directions in the Brillouin zone (see Fig. 4).[17,18)] Table 5 summarizes the relative values of the conduction band widths[19)] ($\Delta W_{\Gamma\text{-Y}}$ and $\Delta W_{\Gamma\text{-X}}$) of α-(BEDT-TTF)$_2PF_6$, EVT$_2PF_6$, EVT$_2AsF_6$, and VT$_2PF_6$. It is noticeable that $\Delta W_{\Gamma\text{-Y}}$ increases in the order α-(BEDT-TTF)$_2$PF$_6$<EVT$_2$PF$_6$<VT$_2$PF$_6$. On the other hand, $\Delta W_{\Gamma\text{-X}}$ changes in the reverse order. Since $\Delta W_{\Gamma\text{-Y}}$ and $\Delta W_{\Gamma\text{-X}}$ are comparable in α-(BEDT-TTF)$_2$PF$_6$, this salt is assumed to possess a two-dimensional electronic property. Table 5 shows that the extent of the two-dimensional nature is largest for α-(BEDT-TTF)$_2$PF$_6$, intermediate for EVT$_2$PF$_6$, and smallest for VT$_2$PF$_6$. The relation between the conduction band widths and the crystal structures are discussed below in more detail regarding these salts.

The $\Delta W_{\Gamma\text{-X}}$ value of α-(BEDT-TTF)$_2$PF$_6$ is the largest among those of the conducting salts given in Table

5. The main reason for this arises from the largest absolute overlap integral $|s|$ of this salt (Table 4). All of the HOMO levels of BEDT-TTF, EVT, and VT have larger LCAO coefficients on the sulfur atoms than those on the carbon atoms. Thus, the overlap integral, *s*, is mainly determined by the side-by-side overlap between the lone-pair orbitals of the sulfur atoms belonging to the adjacent donor columns. The main reason that the $\Delta W_{\Gamma\text{-}Y}$ value for EVT_2PF_6 is larger than that for α-$(BEDT\text{-}TTF)_2PF_6$ arises from the larger value of *q* in the former salt. Here, *q* denotes the intercolumnar molecular overlap integral between the donor molecules related by a symmetry operation $(1-x, -y, -z)$. On the other hand, EVT salts have smaller values of $\Delta W_{\Gamma\text{-}X}$ than that of α-$(BEDT\text{-}TTF)_2PF_6$. Thus, the extent of the two-dimensional nature of the former salts is less than that of the latter. In the case of VT_2PF_6, $\Delta W_{\Gamma\text{-}Y}$ is much larger than those of the corresponding BEDT-TTF and EVT salts. The main reason for this arises from the largest value of *b2* (intracolumnar molecular overlap integral). The mode of the the stacking of the donor molecules connected by the overlap integral *b2* are characterized by l_2 in Table 3. In the case of α-$(BEDT\text{-}TTF)_2PF_6$, the mode of the intermolecular overlap is that of a "ring-external bond-type overlap" usually found in 1-D organic metals. On the other hand, a six-membered ring of one molecule overlaps with a five-membered ring of another molecule in EVT_2PF_6 and VT_2PF_6; the extent of the molecular overlap of the latter salts is larger than that of the former. These features are characterized by the order of l_2 values: α-$(BEDT\text{-}TTF)_2PF_6 > EVT_2PF_6 > VT_2PF_6$. Moreover, only VT_2PF_6 has four S····S contacts shorter than the van der Waals distance between the donor molecules connected by the overlap integral, *b2*. Since the terminal vinylene group of a VT molecule is less sterically crowded than the terminal ethylene group of a BEDT-TTF or an EVT molecule, especially in the presence of PF_6^- anion nearby, the VT molecules related by a symmetry operation $(1-x, -y, -z)$ are stacked more closely than the latter molecules are in EVT_2PF_6 or α-$(BEDT\text{-}TTF)_2PF_6$; this gives rise to the largest value of *b2* for the former salt. On the other hand, the intercolumnar overlap integrals (*p*, *q*, and *s*) of VT_2PF_6 are not very different from the corresponding values of the EVT salt; the $\Delta W_{\Gamma\text{-}X}$ value of VT_2PF_6 is similar to that of the EVT salt. Therefore, the extent of the one-dimensional band electronic property of VT_2PF_6 is the largest among the conducting salts listed in Table 5. Comparing the modes of the molecular overlaps characterized by l_1 values in Table 3, α-$(BEDT\text{-}TTF)_2PF_6$ showed a direct overlap of the molecules; i.e., l_1 is very small (~0.3 Å). On the other hand, EVT_2PF_6 and VT_2PF_6 showed appreciable shifts of the molecules. These molecular overlaps are related to the overlap integral, *b1*. Therefore, *b1* of α-$(BEDT\text{-}TTF)_2PF_6$ is much larger than those of EVT_2PF_6 and VT_2PF_6. However, *b1* does not appear in the equations of the band widths, $\Delta W_{\Gamma\text{-}Y}$ and $\Delta W_{\Gamma\text{-}X}$, but does in the equations for the band gaps.

The electrical conductivities of various VT-salts have been measured, and most of them showed a metal-insulator transition.[20] The temperature dependence of the X-ray crystallographic analysis of VT_2PF_6 revealed a doubling of the lattice constants below 170 K $[(a,b,c) \rightarrow (2a,2b,2c)]$.[20] These results are assumed to be caused by the quasi-one-dimensional nature of the VT-salts. Since the extent of the two-dimensional nature of the EVT-salts is expected to be greater than that of the VT-salts, as in the present study, and since EVT is the molecule with the slightest modification of BEDT-TTF,[3] EVT-salts are expected to give conducting salts with electronic properties similar to those of BEDT-TTF salts. Syntheses of the other conducting EVT-salts are underway using electrochemical crystallization and a diffusion method.

We are grateful to the Protein Engineering Center, Institute for Protein Research, Osaka University, for the use of ACOS S850 Computer.

References

1) *Synth. Met.*, **27**, Nos. 1—4 (1988), Proceedings of the International Conference on Science and Technology of Synthetic Metals (ICSM '88), Santa Fe, NM, USA.

2) H. Kobayashi, R. Kato, A. Kobayashi, Y. Nishio, K. Kajita, and W. Sasaki, *Chem. Lett.*, **1986**, 833; A. Kobayashi, R. Kato, H. Kobayashi, S. Moriyama, Y. Nishio, K. Kajita, and W. Sasaki, *ibid.*, **1987**, 459.

3) H. Nakano, T. Nogami, Y. Shirota, S. Harada, and N. Kasai, *Bull. Chem. Soc. Jpn.*, **62**, 2604 (1989).

4) T. Nakamura, S. Iwasaka, H. Nakano, K. Inoue, T. Nogami, and H. Mikawa, *Bull. Chem. Soc. Jpn.*, **60**, 365 (1987); T. Nakamura, T. Nogami, and Y. Shirota, *ibid.*, **60**, 3447 (1987).

5) T. Mori, A. Kobayashi, Y. Sasaki, H. Kobayashi, G. Saito, and H. Inokuchi, *Bull. Chem. Soc. Jpn.*, **57**, 627 (1984).

6) H. Kobayashi, R. Kato, T. Mori, A. Kobayashi, W. Sasaki, G. Saito, and H. Inokuchi, *Chem. Lett.*, **1983**, 759.

7) H. Kobayashi, A. Kobayashi, T. Nakamura, T. Nogami, and Y. Shirota, *Chem. Lett.*, **1987**, 559.

8) F. Palacio, C. G. Lagrange, L. Brezynski, J. Amiell, J. Gaultier, and P. Delhaes, *Solid State Commun.*, **70**, 717 (1989).

9) P. Main, S. E. Hull, L. Lessinger, G. Germain, J-P. Declercq, and M. M. Woolfson, MULTAN 78, "A System of Computer Programs for the Automatic Solution of Crystal Structures from X-Ray Diffraction Data," Univ. of York, England and Louvain, Belgium (1978).

10) T. Ashida, HBLS V, The Universal Crystallographic Computing System-Osaka, The Computation Center, Osaka University (1979), p. 53.

11) "International Tables for X-Ray Crystallography," Kynoch Press, Birmingham, England (1974), Vol. IV, p. 71.

12) W. C. Hamilton, *Acta Crystallogr.*, **12**, 609 (1959).

13) Tables of anisotropic thermal parameters of nonhydrogen atoms, calculated positional parameters and assumed isotropic thermal parameters of hydrogen atoms, bond distances and angles, and observed and calculated structure factors are kept (as Document No. 8931 both for EVT_2PF_6 and EVT_2AsF_6) at the Office of the Editor of Bull. Chem. Soc. Jpn.

14) The positions of hydrogen atoms were estimated by assuming sp^2 and/or sp^3 hybridizations of terminal carbons of a donor molecule for the computation of the extended Hückel molecular orbitals.

15) Since the band structures of EVT_2PF_6 and EVT_2AsF_6 are very similar, the band structure of EVT_2AsF_6 will not be discussed in detail in this paper.

16) H. Kobayashi, R. Kato, A. Kobayashi, T. Mori, H. Inokuchi, Y. Nishio, K. Kajita, and W. Sasaki, *Synth. Met.*, **27**, A289 (1988).

17) For α-$(BEDT\text{-}TTF)_2PF_6$ and VT_2PF_6, the expressions of the matrix elements can be used if *kc* is replaced by *ka* (see Refs 6 and 7).

18) For α-$(BEDT\text{-}TTF)_2PF_6$ and VT_2PF_6, $\Delta W_{\Gamma\text{-}X}$ should be interpreted as $\Delta W_{\Gamma\text{-}Z}$ (see Refs 6 and 7).

19) Since the transfer integrals t_x (x=*b1*, *b2*, *p*, *q*, and *s*) are of the order of *ES* (E=orbital energy of HOMO level) and the values of E are not very different from one another for BEDT-TTF, EVT, and VT, the relative conduction band widths are shown by adopting the overlap integrals multiplied by 10^3 in Table 4.

20) Unpublished data.